PCCP

Accepted Manuscript

ROYAL SOCIETY OF CHEMISTRY

www.rsc.org/pccp

Journal Name

RSCPublishing

ARTICLE

Distinguishing isobaric phosphated and sulfated carbohydrates by coupling of mass spectrometry with gas phase vibrational spectroscopy

Cite this: DOI: 10.1039/x0xx00000x

Received ooth January 2012,
Accepted ooth January 2012

DOI: 10.1039/x0xx00000x

www.rsc.org/

Baptiste Schindler,[abc] Janhavi Joshi,[abc] Abdul-Rahman Allouche,[abc] Daniel Simon,[abc] Stéphane Chambert,[abd] Vincent Brites,[e] Marie-Pierre Gaigeot[e,f] and Isabelle Compagnon*[abcf]

An original application of the coupling of mass spectrometry with vibrational spectroscopy, used for the first time to discriminate isobaric bioactive saccharides with sulfate and phosphate functional modifications is presented. Whereas their nominal masses and fragmentation patterns are undifferentiated by sole mass spectrometry, their distinctive OH stretching modes at 3595 cm^{-1} and 3666 cm^{-1}, respectively, provide a reliable spectroscopic diagnostic for distinguishing their sulfate or phosphate functionalization. A detailed analysis of the 6-sulfated and 6-phosphated D-glucosamine conformations is presented, together with theoretical scaled harmonic spectra and anharmonic spectra (VPT2 and DFT-based molecular dynamics simulations). Strong anharmonic effects are observed in the case of the phosphated species, resulting in a dramatic enhancement of its phosphate diagnostic mode.

Introduction

Among biomolecules, saccharides display unique structural features, i.e. branched isomers, positional isomers of functional modifications, and the frequent occurrence of isobaric building blocks. Therefore, whereas mass spectrometry (MS) is remarkably efficient to sequence other biopolymers such as proteins and DNA, these sequencing methods cannot be readily transferred to the structural characterization of polysaccharides.[1-4] Development of novel carbohydrate-specific mass spectrometry techniques is hence essential to provide routine analytical methods for the identification of natural saccharides, as well as refined structural characterization tools to unravel their amazing biological versatility. To that end, more sophisticated methods involving the coupling of mass spectrometry with additional, direct structural information are actively developed. Among them, ion mobility[5-26] and laser spectroscopy are particularly promising.

Laser spectroscopy offer the advantage of more structural detail than sole MS: electronic spectroscopy,[27] rotational spectroscopy[28] and vibrational spectroscopy[29-38] of isolated, mass selected carbohydrates building blocks were established in the past few years. The coupling of mass spectrometry with vibrational spectroscopy, which has proven highly efficient for the detailed structural characterization of polypeptides in the past decade,[39-44] was scarcely applied to oligosaccharides. The seminal work of Simons et al. on monosaccharides [32, 33] and oligosaccharides[34-36, 45] demonstrated that gas phase IR spectroscopy is a remarkable tool for the conformational analysis of mass selected oligosaccharides. In particular, stretching and bending modes of OH groups unravel the intramolecular H-bond network responsible for the stability of the 3-dimensional arrangement of biomolecules. The case of isobaric phosphated ($R\text{-}H_2PO_4$) and sulfated ($R\text{-}HSO_4$) compounds is a striking example of analytical issue. Indeed, while they are prevalent in biological processes and abundant in biological tissues, their identical nominal mass and undifferentiated fragmentation pattern leads to ambiguous MS/MS analysis. Hence, specific analytical strategies were actively developed, including Ultra High resolution mass spectrometry[46] and dedicated ion pairing agents. [47-49] In this context, we report here an original application of the coupling of mass spectrometry with vibrational spectroscopy, used for the first time to distinguish functionalized bioactive saccharides of same nominal mass, namely 6-phosphated vs. 6-sulfated

glucosamine. We present an unambiguous vibrational signature for protonated D-Glucosamine 6-Phosphate, which is the natural precursor of nitrogen-containing sugars, and protonated D-Glucosamine 6-Sulfate, which is a building block of glycosaminoglycans.[50] This work opens the way to a general method for the spectroscopic discrimination between sulfated and phosphated polysaccharides isolated from natural samples by mass spectrometry.

Methods

We performed action IR spectroscopy of mass selected, protonated D-Glucosamine 6-Phosphate vs. D-Glucosamine 6-Sulfate in the 3 µm spectral range, corresponding to the excitation of the OH stretching modes, and we focused on the specific optical response of the phosphate vs. sulfate group. For this purpose, we have built a IRMPD setup (Infra Red Multiple Photon Dissociation) similar to that of reference 51. It consists of a commercial 3D-ion trap mass spectrometer (Thermofinnigan LCQ) coupled with an electrospray ionization source (ESI). The spectrometer was modified to allow injecting the laser beam from a YAG-pumped tunable IR OPO/OPA through a sapphire window directly on the cloud of mass-selected ions. Upon resonant IR excitation, the ions undergo fragmentation. A vibrational spectrum is obtained by monitoring the photofragmentation yield as a function of the IR wavelength. More details are given in the Suppl. Material. Complementary experiments were performed in the mid-IR range (5-10 µm) with a similar setup at the CLIO laser facility.[52]

The interpretation of the diagnostic sulfate and phosphate specific modes was supported by state-of-the art vibrational calculations, and analyzed with Gabedit.[53] We have identified the conformations responsible for the vibrational features with DFT (Density Functional Theory) scaled harmonic frequencies. The structures have been generated through an exploration of the potential energy surface by molecular dynamics simulations. See details in the Suppl. Mat. Note that both α and β-anomers were addressed for each molecule, as they co-exist in the sample. We have subsequently refined the interpretation of the vibrational features with anharmonic frequency calculations, either in the form of VPT2[54] or DFT-based molecular dynamics simulations (DFT-MD).[55] More details can be found in the Suppl. Mat.

Results and discussion

Mass spectrometry

The nominal masses of D-Glucosamine 6-Phosphate ($C_6H_{14}NO_8P$) and D-Glucosamine 6-Sulfate ($C_6H_{13}NO_8S$) are 259 amu, which result in an identical peak at 260 amu for the protonated parent ion in both individual mass spectra shown in Fig. 1. Under soft collision conditions (CID), both species undergo a neutral loss of 18 amu resulting in an identical fragment peak at 242 amu. This identical second reaction monitoring (SRM) transition is typical of sulfated and phosphated compounds and results in a critical uncertainty in routine MS/MS analysis of such compounds. Note that the isotopic masses of the protonated ions are not exactly equal: 260.0535 and 260.0440, respectively. This mass difference of 0.0094 amu[46] corresponds to a mass resolution of ca. 28,000 for monosaccharides and exceeds 100,000 for pentasaccharides. It could hence only be differentiated using ultra high resolution mass spectrometry instruments.

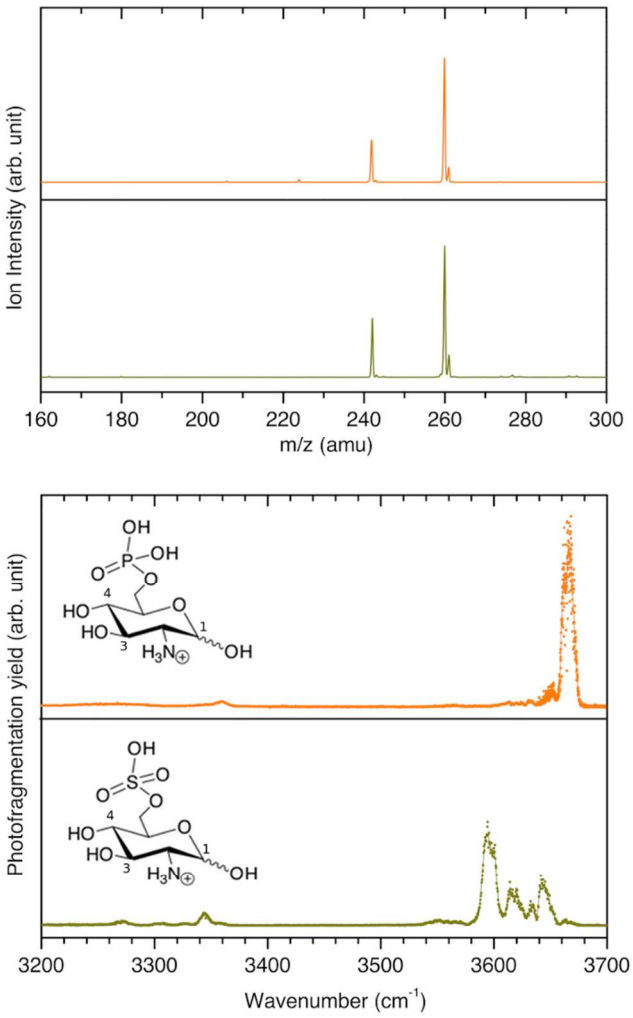

Fig. 1 Top panel: MS/MS spectrum of Glucosamine 6-Phosphate (orange) and Glucosamine 6-Sulfate (dark yellow). Lower panel: IRMPD spectrum of Glucosamine 6-Phosphate (orange) and Glucosamine 6-Sulfate (dark yellow). Insets: structure of the respective pyranose forms.

Spectroscopic discrimination of sulfated and phosphated groups

The individual action vibrational spectra of Glucosamine 6-Phosphate and Glucosamine 6-Sulfate recorded in the OH stretching region are shown in Fig. 1. While they have an undifferentiated MS signature, their vibrational spectra are distinct. Both species display two main regions of vibrational activity around 3650 cm^{-1} and 3300 cm^{-1}, corresponding to the typical spectral ranges of free OH stretching modes and protonated amine (NH_3^+) stretching modes, respectively. The vibrational spectra of the two species are clearly distinctive in

the region of free OH stretches: the spectrum of Glucosamine 6-Phosphate is indeed dominated by one single intense feature at 3666 cm^{-1}, whereas the spectrum of Glucosamine 6-Sulfate displays a broad active region between 3580 and 3675 cm^{-1}, with the most intense feature at 3595 cm^{-1}. Additionally, the complementary measurements in the mid-IR region (Fig. S1 in Supp. Mat.) reveal no activity in the spectral region of the C=O stretching (around 1700 cm^{-1}).

These spectroscopic observations readily offer a diagnostic for the main structural features of the species. Firstly, the bands observed in the 3300 cm^{-1} region are typical of a NH_3^+ group and are interpreted as the protonation of the amine group, in agreement with its relative acidity. Secondly, the question of linear vs. cyclic form of monosaccharide ions in the gas phase has been raised by the work of Bendiak et. al., who found a significant amount of open-chain configurations in the case of isolated deprotonated aldohexoses, including glucose,[56] via the observation of a free carbonyl stretching mode around 1700 cm^{-1}. In our case, such diagnostic mode was not observed, which provides a strong evidence for the presence of a cyclic form as the major component of the protonated ions. Hence it appears that the pyranose form of the glucosamine, which is the most abundant in solution, is preserved under protonation and transferred to the gas phase. Finally, the spectra of the phosphated and sulfated species are distinctive in the 3600 cm^{-1} region, especially with the presence of intense features located 71 cm^{-1} apart, respectively at 3666 cm^{-1} and 3595 cm^{-1}: this offers a non ambiguous spectroscopic diagnostic of phosphated and sulfated saccharides, respectively, in agreement with the findings of Polfer et. al. concerning sulfo- and phosphopeptides.[57]

In order to evaluate the robustness of this vibrational diagnostic, the position of the sulfate and phosphate OH stretching modes was calculated for a large number of conformers. Based on the experimental results above, the conformational search was restricted to four pyranose structures, namely α-D-Glucosamine 6-Phosphate, β-D-Glucosamine 6-Phosphate, α-D-Glucosamine 6-Sulfate, β-D-Glucosamine 6-Sulfate, with a fixed protonation site on the amine function. Circa 200 conformations were obtained for each of the 4 ions of interest within an energy range of 25 kJ/mol, and were further analyzed with scaled harmonic frequencies. The positions of the diagnostic modes, i.e. sulfate OH and two phosphate OH stretches are reported in Fig. 2. The striking result is that these modes are unrelated to the structure or to the anomeric configuration. All families of conformations indeed exhibit a sulfate OH stretching mode around 3590 cm^{-1}, or two phosphate OH stretching modes in the narrow range 3650-3680 cm^{-1}. There is furthermore no overlap in the frequency domains between sulfate and phosphate groups. Note also that these scaled harmonic frequencies match well the experimental values. They hence provide a reliable, anomer- and conformation-independent diagnostic of the phosphated or sulfated nature of the saccharide.

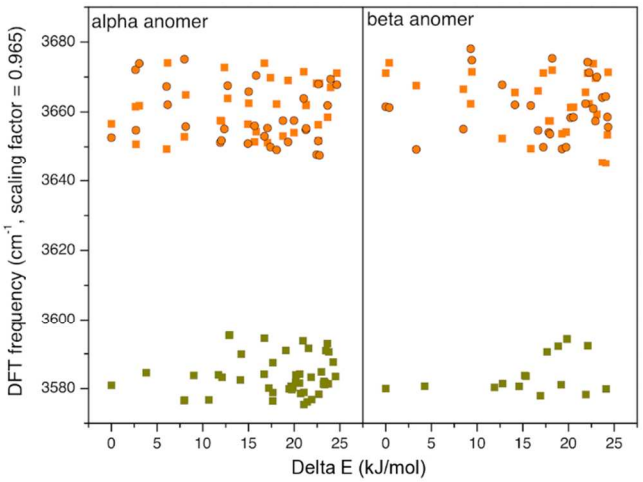

Fig. 2 Calculated scaled harmonic DFT frequencies of the sulfate OH stretch (dark yellow squares) and the phosphate OH pair stretches (orange squares and circles) for all conformers identified by exploration of the potential energy surfaces of Glucosamine 6-Phosphate and Glucosamine 6-Sulfate. These structures are within an energy range of 25 kJ/mol.

Assignment of structures responsible for the IR-MPD signatures

The conformers mentioned above were fully analyzed in terms of conformation of the pyranose ring and H-bond interactions between the phosphate (or sulfate) and the carbohydrate hydroxyl functions of the ring. They are shown in insets in Fig. 3 together with their scaled harmonic spectra. Our goal is to use these calculated harmonic spectra for the assignment of the structures of the saccharides, by comparison to the experiment.

For both sulfated and phosphated species, α and β-anomers adopt the $^4C_1$ chair conformation as the lowest energy structure with variations in the orientation of the function with respect to the pyranose ring, resulting in conformers within roughly 16 kJ/mol (Fig. 3). Three types of function/ring interactions are observed: (i) an oxygen of the function is H-bonded to the OH(4) of the sugar ring, (ii) an oxygen of the function is H-bonded to the OH(1) of the ring, (iii) the function presents no interaction with the carbohydrate's OH (only observed for α-anomers). Two other ring conformations are observed for α-anomers only: a $^1C_4$ chair presenting a H-bond between an oxygen of the function and OH(3) at low energy and a boat ^{3,0} with a H-bond between an oxygen of the function and OH(4) at higher energy (shown in Fig. 3). Additional minor conformers are shown in Fig. S2 in Supp. Mat.

For all forms, the H-bond may involve any one of the three types of oxygen atom present in the sulfate or phosphate function (i.e. X=O, X-OH, C-O-X with X=S or P). However, the binding of a X=O oxygen results into stronger H-bonds, consequently yielding lower energy structures. Only these strongly H-bonded structures are shown in Fig. 3 for clarity.

The scaled harmonic spectra of these conformations are presented in the 2850-3700 cm^{-1} spectral range in Fig. 3 and offer a wealth of structural diagnostic. The OH, NH and CH stretching modes are color-coded to aid analysis, see Fig. caption.

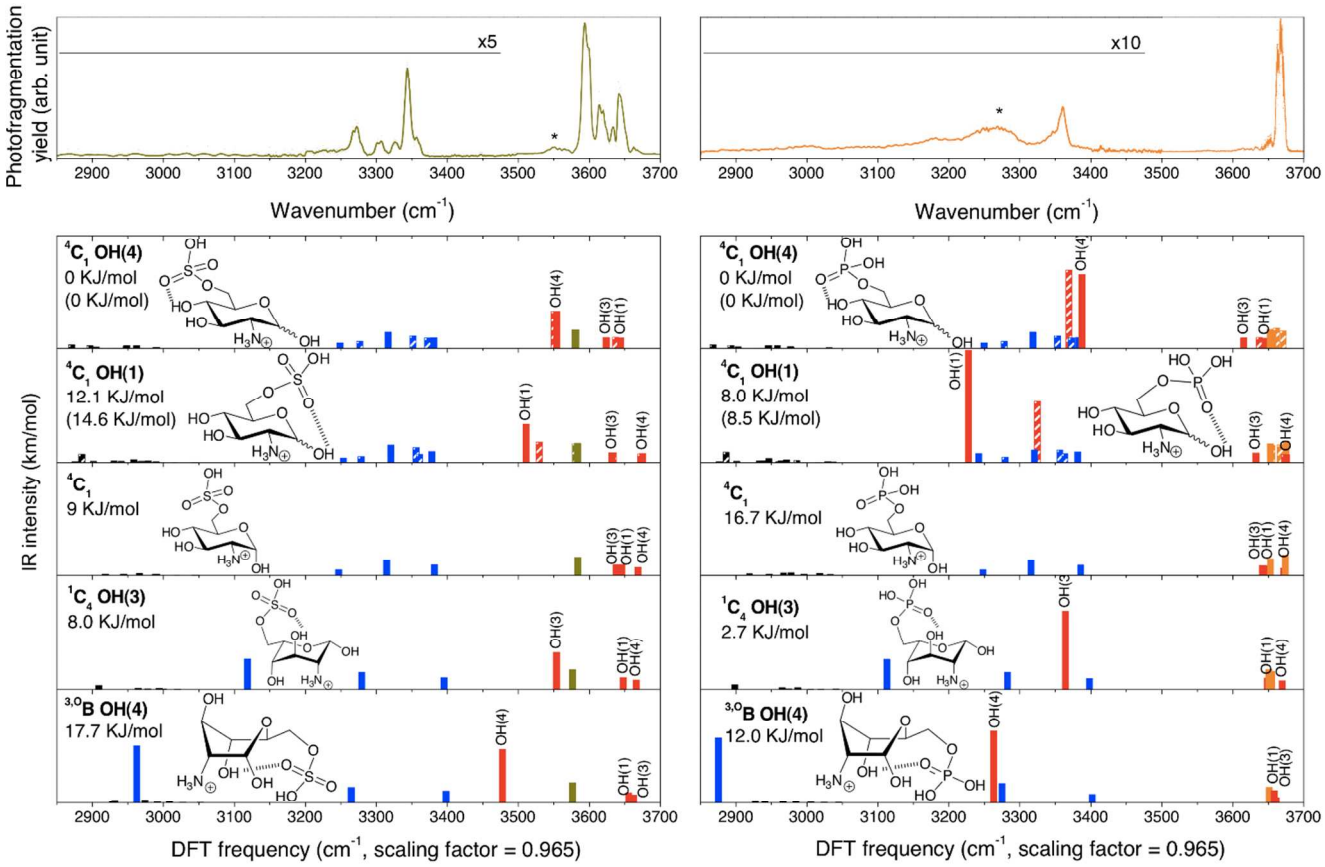

Fig. 3 Experimental (top panel) and calculated (lower panel) IR spectra. Scaled harmonic vibrational frequencies obtained with DFT B3LYP/6-311+G* for the lowest energy conformations of Glucosamine 6-Sulfate (left panel) and Glucosamine 6-Phosphate (right panel). Structures and relatives energies are given in inset (energies of β-anomers in brackets when both are present). A color code is used to highlight the mode analysis: OH stretch from groups of Phosphate and Sulfate functions are reported in orange and dark yellow, respectively. NH's are reported in blue, carbohydrate OH's in red with individual labels indicating their position on the pyranose ring, and CH's in black. Solid bars are used to represent α-anomers, and dashed bars are used to represent β-anomers.

First, the triplet of NH stretching modes of the protonated amine group (blue bars in Fig. 3), which consists of one low frequency symmetric stretch and two higher energy asymmetric stretches, provides an interesting ring conformation-specific signature. (i) the form $^4C_1$ maintains a minimal interaction environment for the NH_3^+ group, due to the equatorial orientations of NH_3^+, OH(3) and OH(4). This results in a characteristic, compact 3-bands pattern between 3250 and 3280 cm^{-1}, as observed in Fig. 3 (top 1st, 2d and 3rd panels). Note that for the α-anomer, the symmetric NH_3^+ stretch is typically red-shifted by 25 cm^{-1} as compared to the β-anomer. This is explained by an increased interaction between NH_3^+ and OH(1) in axial position (α-anomer) as compared to OH(1) in equatorial position (β-anomer). Axial vs. equatorial interactions were previously addressed by Çarçabal et.al. with similar conclusions.[58] (ii) For the $^1C_4$ chair, the NH_3^+ and OH(4) groups are brought in close proximity, in axial position under the plane of the ring. This configuration constitutes an intermediate regime of interaction for the protonated amine, where OH(4) is H-bonded to NH_3^+, causing a red-shift of the symmetric stretch to 3100 cm^{-1} and resulting in a spreading of the NH_3^+ modes pattern. (iii) The boat $^{3,O}B$ form provides the highest interaction environment for the NH_3^+ group, which forms H-bonds with both OH(1) and OH(4). The resulting NH_3^+ pattern is further spread towards the low frequencies, with a symmetric mode red-shifted below 3000 cm^{-1}.

Secondly, the observation of the pattern formed by the three ring OH's (red bars in Fig. 3) clarifies the type of interaction between the function and the ring. Indeed, in absence of interaction a very compact pattern of 3 free OH stretching modes is observed around 3650 cm^{-1}, whereas a H-bond formed between a sulfate or phosphate oxygen and a ring OH results in a considerable red-shift of the OH stretch. Typical position of the H-bonded ring OH stretch ranges between 3470 and 3550 cm^{-1} in case of the sulfated species, which typically falls between the sulfate OH stretching mode (dark yellow bars in Fig. 3) and the NH_3^+ pattern. For phosphated species, the H-bonded ring OH stretching frequency is even more red-shifted and falls somewhere in the NH_3^+ pattern.

Finally, we used these harmonic spectra to assign the IRMPD features (top panel of Fig. 3). Note that, this assignment is based on the identification of spectroscopic patterns rather than on the absolute position of the bands. For this purpose, a generic factor of 0.965 was used to scale down the computed

harmonic frequencies, without attempting to minimize the deviation to the experimental spectra.

For Glucosamine 6-Sulfate, the best agreement between experiment and theory is obtained for the lowest energy structure, i.e. a mixture of α and β-anomers in a $^4C_1$ chair conformation with the sulfate group in H-bond interaction with OH(4). Indeed, (i) the distinctive, compact NH_3^+ pattern of the $^4C_1$ chair matches the experiment around 3300 cm^{-1} and (ii) the broad feature marked with a star in the experimental spectrum, which is typical from a H-bonded mode, matches the predicted position of the H-bonded OH(4) band. The other carbohydrate OH's were not primarily used for the structural assignment. Nevertheless, their calculated positions are consistent with the experimental pattern around 3650 cm^{-1}, which further support our conclusion. As discussed above, the sulfate OH stretching mode is a robust diagnostic of the presence of the sulfate function, as its calculated position is anomer- and conformation-independent. It shows an excellent agreement with the most intense peak in the experimental spectrum at 3595 cm^{-1}. Note that the deviation could be further minimized by using a scaling factor of 0.968.

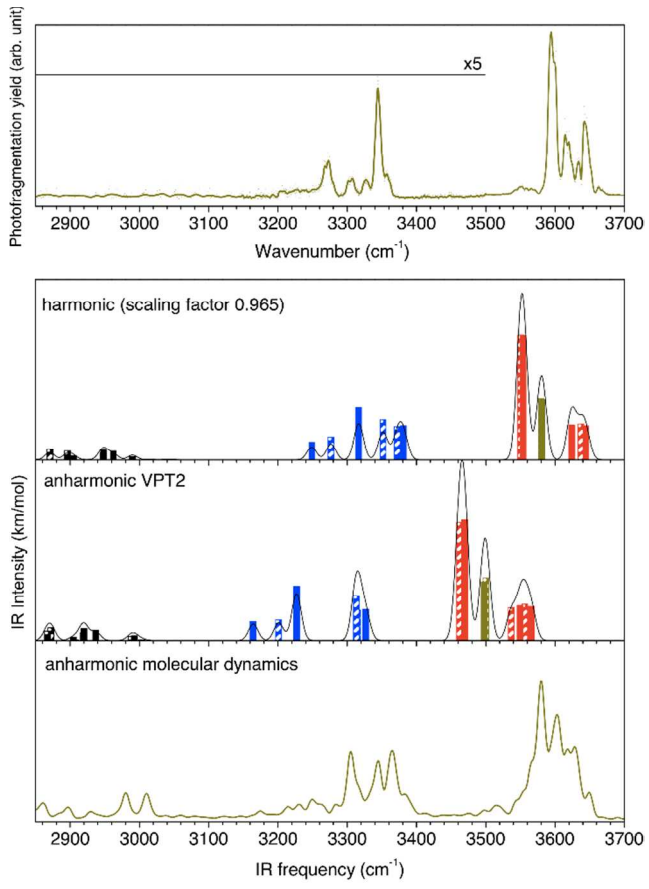

Fig. 4 Experimental IRMPD spectrum of Glucosamine 6-Sulfate (top panel) compared with harmonic and anharmonic simulations (lower panel, see detail in the text). See Fig. 3 caption for color code.

The assignment of the Glucosamine 6-Phosphate structure is complicated by the very intense feature at 3666 cm^{-1} in the experimental spectrum, which hinders all other spectral features. As in the case of Glucosamine 6-Sulfate, this dominant feature is consistent with the calculated position of the two phosphate OH stretching modes. As for Glucosamine 6-Sulfate, the active region around 3300 cm^{-1} is consistent with the NH_3^+ pattern of a $^4C_1$ chair, superimposed with a broadened H-bonded ring OH stretching mode (marked with a star in Fig. 3). Based on the energetics of the calculated structures, it seems reasonable to assign the experimental data to the lowest energy structure, i.e. a $^4C_1$ chair with a phosphate/carbohydrate OH(4) interaction, despite a poor agreement on the calculated position of the latest.

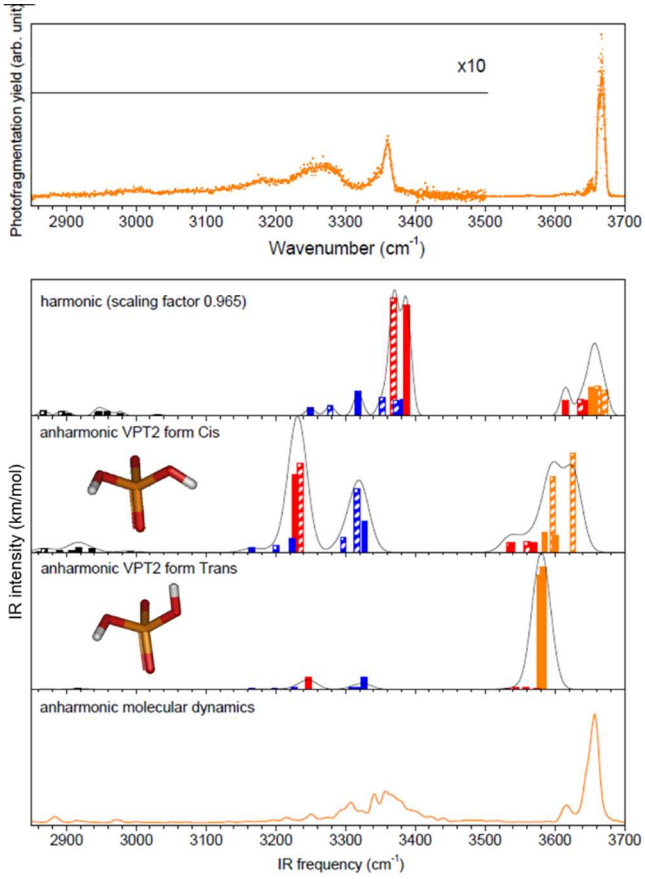

Fig. 5 Experimental IRMPD spectrum of Glucosamine 6-Phosphate (top panel) compared with harmonic and anharmonic simulations (lower panel, see detail in the text). Intensities are normalized on the most intense peak. See Fig. 3 caption for color code.

Anharmonic spectra and final assessment of structural assignments

The question of anharmonic effects in saccharides has been addressed by Gerber et. al.[37,59] Here, while a good match was obtained for the overall spectrum of the lowest energy structure for Glucosamine 6-Sulfate, the calculated scaled harmonic spectra are not as satisfactory in the case of Glucosamine 6-Phosphate. Indeed, (i) none of the calculated harmonic spectra account for the remarkably high intensity of the phosphate OH peak observed experimentally and (ii) the position of the H-bonded OH(4) mode is poorly reproduced. In order to

investigate these two issues, anharmonic calculations were performed on the lowest energy structure for both sulfate and phosphate species (α and β-anomers). We compare two theoretical approaches: VPT2 and finite temperature molecular dynamics anharmonic IR spectra. See Figs. 4-5.

The dynamical anharmonic spectra are calculated through Born-Oppenheimer DFT-based molecular dynamics simulations, following our established procedure.[55] 8 ps dynamics at a temperature of 300 K, corresponding to experimental conditions, have been performed. We insist that the IR dynamical anharmonic spectra presented in Figs. 4-5 (bottom panels) have no scaling factors nor frequency shifts applied. The sampling of vibrational anharmonicities, i.e. potential energy surface, dipole anharmonicities, mode couplings, anharmonic modes, being included in our simulations by construction, application of scaling factors to the band positions is therefore not required. Note that we present the sums of α and β-anomers in the dynamical spectra in order to account for their mixture in the experiment.

Whereas the frequencies are typically underestimated by the harmonic frequencies and are scaled down with an empirical factor of 0.965, they tend to be overestimated by VPT2 calculations for both molecules. Using the molecular dynamics method, the agreement between the dynamical anharmonic spectra and the IRMPD experiments is excellent for both molecules, in terms of band-positions, intensities and shapes. The mean deviation between the dynamical anharmonic spectra and the experiments is respectively +10 cm^{-1} for Glucosamine 6-Phosphate and +14 cm^{-1} for Glucosamine 6-Sulfate, based on the free OH stretches. This deviation is of the order of magnitude of the experimental resolution.

For Glucosamine 6-Sulfate, VPT2 calculations result in a bare 50 cm^{-1} red-shift of the overall harmonic spectrum with small differences for the band gaps and relative intensities, as seen in Fig. 4. This indicates that the anharmonic effects are weak if any. The dynamical spectrum provides an excellent match for band positions, shapes and relative intensities. In particular, the broadening of the H-bonded ring OH(4) is very nicely reproduced, yielding the feature at 3510 cm^{-1} (exp: 3550 cm^{-1})

The case of Glucosamine 6-Phosphate is more revealing of anharmonicities. Cis and Trans orientations of the phosphate OH's were found in the optimized structures within <3 kJ/mol, hence very likely coexisting at room temperature, and resulted in virtually identical harmonic spectra. (Only the spectra of the Trans form were shown in Fig. 3, for clarity). However, the analysis of the modes revealed that the two phosphate OH stretching vibrations are individual in the Cis form, but are coupled in the Trans form, resulting in a symmetric and an antisymmetric stretching modes. Interestingly, the VPT2 spectra of these two forms are different, as shown in Fig. 5, and strong anharmonic effects are present: the NH_3^+ pattern is significantly affected by the anharmonic corrections, with a change in relative intensities. More strikingly, the H-bonded OH(4) stretching mode is markedly red-shifted from the harmonic calculation, and now matches the experiment. The main difference between the Cis and Trans forms lies in the changes of intensity of the Phosphate mode: it is dramatically enhanced and now dominates the rest of the spectrum for the Trans form, as observed experimentally, and is only mildly enhanced for the Cis form (the intensities in Fig. 5 are normalized on the most intense peak). In the likely hypothesis of a mixture of both forms present in the sample, the strong anharmonic feature of the Trans form is dominant, which results in a very satisfactory overall agreement of the VPT2 spectrum with the experimental spectrum of the Glucosamine 6-Phosphate.

The view provided by the dynamics is that, at 300 K, the $^4C_1$ ring conformation is preserved, as well as the H-bonding of OH(4) throughout the entire trajectory, while there is a continuous rotational motion of the two OH's of the phosphate at the finite temperature of the IRMPD experiment, as already observed in a previous work.[60] They rotate freely at room temperature, allowing rapid and continuous inter-conversions between Cis and Trans forms orientations (see details in Suppl. Mat.). As a consequence, the Glucosamine 6-Phosphate saccharide cannot be considered as a rigid molecule from the point of view of the phosphate function (fixed either in a Cis or Trans form), but instead as dynamical. When this is taken into account in the anharmonic dynamical spectrum calculation, as shown in Fig. 5, one obtains an excellent agreement with the experiment, not only for the phosphate modes but also for the mixture of NH and broad OH modes around 3300 cm^{-1}, matching the experiment for band positions and intensities.

A detailed analysis of the evolution with time of H-bonds furthermore provides understanding of the large red-shift of the OH(4) stretch observed in the spectrum of Glucosamine 6-Phosphate in comparison to Glucosamine 6-Sulfate (See Suppl. Mat. for details and figures). The evolution with time of the OH(4)…O=X reveals: (i) no drastic difference between α and β-anomers for one given species, (ii) the average H-bond distance is about 1.9 Å in the phosphated species whereas it is slightly longer and about 2.1 Å for the sulfated one, (iii) the fluctuations in distance are also different between both species, the maximum distance reaches about 2.6-2.7 Å for α-/β-Glucosamine 6-Phosphate, and about 2.9-3.0 Å for α-/β-Glucosamine 6-Sulfate. Based on distances criteria, the H-bond in Glucosamine 6-Phosphate thus appears stronger, leading to the OH(4) stretching mode located around 3300 cm^{-1}, while the H-bond in Glucosamine 6-Sulfate is weaker in strength. This results into an OH(4) band located around 3550 cm^{-1}, weakly red-shifted from free OH stretches.

Conclusion

It appears clearly that, the vibrational spectroscopy of phosphated and sulfated glucosamine in the 3 μm region provides a very distinctive and robust diagnostic for the nature of the functional group in isobaric saccharides. By combining IRMPD vibrational experiments on mass selected protonated ions with harmonic and anharmonic frequency calculations, we have shown that: 1) the free OH stretching modes of the phosphate and sulfate functions provide the most intense

feature of the experimental spectra at 3666 cm^{-1} and 3595 cm^{-1}, respectively, which can be used as a robust spectroscopic diagnostic of the function, since it is anomer- and conformer-independent. 2) a theoretical scaled harmonic spectrum provides a very good agreement in band-positions in comparison to the IRMPD spectrum of Glucosamine 6-Sulfate. The vibrational motions in this molecule are thus essentially harmonic, even for the OH(4) which is hydrogen bonded to one O=S of the sulfate function. This is not valid anymore for Glucosamine 6-Phosphate, where the remarkable intensity of the Phosphate OH modes is only accounted for by anharmonic simulations. 3) For both Glucosamine 6-Sulfate and Glucosamine 6-Phosphate molecules, the VPT2 anharmonic frequencies are still too much red-shifted from the experiment and fail at representing the broadening of the H-bonded modes. In contrast, the dynamical anharmonic spectra are strikingly matching the experimental IRMPD, in terms of band-positions, intensities and shapes. In particular, the relative positions of the OH(4) stretch and NH_3^+ stretches match remarkably well the experiments, with a mean deviation of only 10-14 cm^{-1}, similar to the experimental precision. Also of great relevance for the spectral features is the dynamical behavior of the two OH's of the phosphate group at room temperature, which is found to be responsible for the enhancement of the Phosphate OH bands.

The discrimination between isobaric saccharides constitutes an original application of the coupling of mass spectrometry with gas phase vibrational spectroscopy. We have demonstrated here that we have state-of-the art experimental and theoretical tools ready to be applied to that end. Demonstration has been achieved on sulfated and phosphated monosaccharides. This work will be extended to the characterization of anomers and positional isomers in the context of a more general project on the structural characterization of polysaccharides of increasing complexity. DFT-MD dynamical anharmonic theoretical spectroscopy will in particular be readily applicable to more complex systems of increasing size.

Acknowledgements

Financial support was provided by Fédération de recherche André-Marie Ampère, Université Lyon 1 and Institut Universitaire de France. This works was performed using High-Performance Computing Resources from GENCI-CINES (Grant 2013-2014 [087025]). Experiments in the mid-IR region were performed at the free electron laser facility CLIO at Orsay with the support of the TGE «Spectrométrie de masse FT-ICR à très haut champ» funded by the CNRS Institute of Chemistry, and the help of Edith Nicole.

Isabelle Compagnon thanks Pr. Perdita Barran, Bob Boughtflower and Pr. Antony Stace for generous equipment donations, and Serge Martin (ANR TRICO) and Franck Lépine (ANR MUSES) for instrumental support. We thank the technical and administrative support in Lyon: Jacques Maurelli, Marc Barbaire, Christian Clavier, Fransisco Pinto, Sad Mezzour and Claude Lesage. Last but not least, thank you Daddy for driving all the way to Scotland and back to Lyon to bring me the mass spectrometer.

Notes and references

[a] Université de Lyon, F-69622, Lyon, France
[b] Université Lyon 1, Villeurbanne, France
[c] Institut Lumière Matière, UMR5306 Université Lyon 1-CNRS, Université de Lyon 69622 Villeurbanne cedex, France
[d] Laboratoire de Chimie Organique et Bioorganique, INSA Lyon, Bât. J. Verne, 20 Avenue A. Einstein, 69621 Villeurbanne Cedex , CNRS, UMR5246, ICBMS
[e] LAMBE UMR 8587 CNRS, Laboratoire Analyse et Modélisation pour la Biologie et l'Environnement, Université d'Evry Val d'Essonne, 91025 Evry, France.
[f] Institut Universitaire de France IUF, 103 Blvd St Michel, 75005 Paris, France
*isabelle.compagnon@univ-lyon1.fr

† The supplementary material supplied in Supporting Information includes: further detail on experimental and theoretical methods; mid-IR measurements; additional conformers; molecular dynamics figures.

1 M. J. Kailemia, L. R. Ruhaak, C. B. Lebrilla and I. J. Amster, *Anal. Chem.*, 2014, **86**, 196-212.
2 D. J. Harvey, *Mass Spectrom. Rev.*, 1999, **18**, 349-450.
3 J. Zaia, *Omics-a Journal of Integrative Biology*, 2010, **14**, 401-418.
4 J. Zaia, *Mass Spectrom. Rev.*, 2004, **23**, 161-227.
5 S. Lee, T. Wyttenbach and M. T. Bowers, *Int. J. Mass Spectrom.*, 1997, **167**, 605-614.
6 Y. S. Liu and D. E. Clemmer, *Anal. Chem.*, 1997, **69**, 2504-2509.
7 D. S. Lee, C. Wu and H. H. Hill, *J. Chromatogr. A*, 1998, **822**, 1-9.
8 W. Gabryelski and K. L. Froese, *J. Am. Soc. Mass Spectrom.*, 2003, **14**, 265-277.
9 B. H. Clowers, P. Dwivedi, W. E. Steiner, H. H. Hill and B. Bendiak, *J. Am. Soc. Mass Spectrom.*, 2005, **16**, 660-669.
10 J. Zaia, I. Campuzano, K. Giles, R. Bateman, C. Keith and C. E. Costello, *Glycobiology*, 2006, **16**, 1140-1140.
11 P. Dwivedi, B. Bendiak, B. H. Clowers and H. H. Hill, *J. Am. Soc. Mass Spectrom.*, 2007, **18**, 1163-1175.
12 L. S. Fenn and J. A. McLean, *Chem. Commun.*, 2008, 5505-5507.
13 M. D. Plasencia, D. Isailovic, S. I. Merenbloom, Y. Mechref and D. E. Clemmer, *J. Am. Soc. Mass Spectrom.*, 2008, **19**, 1706-1715.
14 T. Yamagaki and A. Sato, *Anal. Sci.*, 2009, **25**, 985-988.
15 M. L. Zhu, B. Bendiak, B. Clowers and H. H. Hill, *Anal. Bioanal. Chem.*, 2009, **394**, 1853-1867.
16 B. C. Bohrer and D. E. Clemmer, *J. Am. Soc. Mass Spectrom.*, 2011, **22**, 1602-1609.
17 L. S. Fenn and J. A. McLean, *Physical Chemistry Chemical Physics*, 2011, **13**, 2196-2205.
18 M. Fasciotti, G. B. Sanvido, V. G. Santos, P. M. Lalli, M. McCullagh, G. F. de Sa, R. J. Daroda, M. G. Peter and M. N. Eberlin, *J. Mass Spectrom.*, 2012, **47**, 1643-1647.
19 D. J. Harvey, C. A. Scarff, M. Crispin, C. N. Scanlan, C. Bonomelli and J. H. Scrivens, *J. Am. Soc. Mass Spectrom.*, 2012, **23**, 1955-1966.
20 H. L. Li, K. Giles, B. Bendiak, K. Kaplan, W. F. Siems and H. H. Hill, *Anal. Chem.*, 2012, **84**, 3231-3239.
21 Y. Seo, A. Andaya and J. A. Leary, *Anal. Chem.*, 2012, **84**, 2416-2423.

22 H. L. Li, B. Bendiak, W. F. Siems, D. R. Gang and H. H. Hill, *Anal. Chem.*, 2013, **85**, 2760-2769.

23 H. L. Li, B. Bendiak, W. F. Siems, D. R. Gang and H. H. Hill, *Rapid Communications in Mass Spectrometry*, 2013, **27**, 2699-2709.

24 K. Pagel and D. J. Harvey, *Anal. Chem.*, 2013, **85**, 5138-5145.

25 P. Both, A. P. Green, C. J. Gray, R. Sardzik, J. Voglmeir, C. Fontana, M. Austeri, M. Rejzek, D. Richardson, R. A. Field, G. Widmalm, S. L. Flitsch and C. E. Eyers, *Nature Chemistry*, 2014, **6**, 65-74.

26 S. Lee, S. J. Valentine, J. P. Reilly and D. E. Clemmer, *Int. J. Mass Spectrom.*, 2012, **309**, 161-167.

27 A. Racaud, R. Antoine, L. Joly, N. Mesplet, P. Dugourd and J. Lemoine, *J. Am. Soc. Mass Spectrom.*, 2009, **20**, 1645-1651.

28 E. J. Cocinero, A. Lesarri, P. Ecija, F. J. Basterretxea, J. U. Grabow, J. A. Fernandez and F. Castano, *Angewandte Chemie-International Edition*, 2012, **51**, 3119-3124.

29 E. B. Cagmat, J. Szczepanski, W. L. Pearson, D. H. Powell, J. R. Eyler and N. C. Polfer, *Physical Chemistry Chemical Physics*, 2010, **12**, 3474-3479.

30 C. S. Contreras, N. C. Polfer, J. Oomens, J. D. Steill, B. Bendiak and J. R. Eyler, *Int. J. Mass Spectrom.*, 2012, **330-332**, 285-294.

31 N. C. Polfer, J. J. Valle, D. T. Moore, J. Oomens, J. R. Eyler and B. Bendiak, *Anal. Chem.*, 2006, **78**, 670-679.

32 F. O. Talbot and J. P. Simons, *Physical Chemistry Chemical Physics*, 2002, **4**, 3562-3565.

33 R. A. Jockusch, F. O. Talbot and J. P. Simons, *Physical Chemistry Chemical Physics*, 2003, **5**, 1502-1507.

34 R. A. Jockusch, R. T. Kroemer, F. O. Talbot, L. C. Snoek, P. Carcabal, J. P. Simons, M. Havenith, J. M. Bakker, I. Compagnon, G. Meijer and G. von Helden, *Journal of the American Chemical Society*, 2004, **126**, 5709-5714.

35 P. Carcabal, I. Hunig, D. P. Gamblin, B. Liu, R. A. Jockusch, R. T. Kroemer, L. C. Snoek, A. J. Fairbanks, B. G. Davis and J. P. Simons, *Journal of the American Chemical Society*, 2006, **128**, 1976-1981.

36 J. P. Simons, E. C. Stanca-Kaposta, E. J. Cocinero, B. Liu, B. G. Davis, D. P. Gamblin and R. T. Kroemer, *Physica Scripta*, 2008, **78**.

37 B. Brauer, M. Pincu, V. Buch, I. Bar, J. P. Simons and R. B. Gerber, *J. Phys. Chem. A*, 2011, **115**, 5859-5872.

38 E. J. Cocinero, P. Carcabal, T. D. Vaden, J. P. Simons and B. G. Davis, *Nature*, 2011, **469**, 76-U1400.

39 C. N. Stedwell, J. F. Galindo, A. E. Roitberg and N. C. Polfer, *Annual Review of Analytical Chemistry, Vol 6*, 2013, **6**, 267-285.

40 M. S. de Vries and P. Hobza, in *Annual Review of Physical Chemistry*, 2007, vol. 58, pp. 585-612.

41 J. P. Simons, *Mol. Phys.*, 2009, **107**, 2435-2458.

42 R. Weinkauf, J. P. Schermann, M. S. de Vries and K. Kleinermanns, *European Physical Journal D*, 2002, **20**, 309-316.

43 N. C. Polfer and J. Oomens, *Mass Spectrom. Rev.*, 2009, **28**, 468-494.

44 J. P. Simons, *Physical Chemistry Chemical Physics*, 2004, **6**, E7-E7.

45 C. S. Barry, E. J. Cocinero, P. Çarçabal, D. P. Gamblin, E. C. Stanca-Kaposta, S. M. Remmert, M. a. C. Fernández-Alonso, S. Rudić, J. P. Simons and B. G. Davis, *Journal of the American Chemical Society*, 2013, **135**, 16895-16903.

46 R. E. Bossio and A. G. Marshall, *Anal. Chem.*, 2002, **74**, 1674-1679.

47 Y. Zhang, E. P. Go, H. Jiang and H. Desaire, *J. Am. Soc. Mass Spectrom.*, 2005, **16**, 1827-1839.

48 Y. Zhang, H. Jiang, E. P. Go and H. Desaire, *J. Am. Soc. Mass Spectrom.*, 2006, **17**, 1282-1288.

49 D. J. Harvey and G. R. Bousfield, *Rapid Communications in Mass Spectrometry*, 2005, **19**, 287-288.

50 C. Westling and U. Lindahl, *Journal of Biological Chemistry*, 2002, **277**, 49247-49255.

51 B. Chiavarino, M. E. Crestoni, S. Fornarini, S. Taioli, I. Mancini and P. Tosi, *Journal of Chemical Physics*, 2012, **137**.

52 P. Maitre, S. Le Caer, A. Simon, W. Jones, J. Lemaire, H. N. Mestdagh, M. Heninger, G. Mauclaire, P. Boissel, R. Prazeres, F. Glotin and J. M. Ortega, *Nuclear Instruments & Methods in Physics Research Section a-Accelerators Spectrometers Detectors and Associated Equipment*, 2003, **507**, 541-546.

53 A. R. Allouche, *Journal of Computational Chemistry*, 2011, **32**, 174-182.

54 V. Barone, *Journal of Chemical Physics*, 2005, **122**.

55 M. P. Gaigeot, *Physical Chemistry Chemical Physics*, 2010, **12**, 3336-3359.

56 D. J. Brown, S. E. Stefan, G. Berden, J. D. Steill, J. Oomens, J. R. Eyler and B. Bendiak, *Carbohydrate Research*, 2011, **346**, 2469-2481.

57 A. L. Patrick, C. N. Stedwell and N. C. Polfer, *Anal. Chem.*, 2014, **86**, 5547-5552.

58 P. Carcabal, T. Patsias, I. Hunig, B. Liu, C. Kaposta, L. C. Snoek, D. P. Gamblin, B. G. Davis and J. P. Simons, *Physical Chemistry Chemical Physics*, 2006, **8**, 129-136.

59 L. Jin, J. P. Simons and R. B. Gerber, *J. Phys. Chem. A*, 2012, **116**, 11088-11094.

60 A. Cimas, P. Maitre, G. Ohanessian and M. P. Gaigeot, *Journal of Chemical Theory and Computation*, 2009, **5**, 2388-2400.